

1 **Effect of knee joint loading on chondrocyte mechano-vulnerability and severity of post-traumatic**  
2 **osteoarthritis induced by ACL-injury in mice**

3

4 Alexander Kotelsky<sup>1,2,3</sup>, Anissa Elahi<sup>4</sup>, Nejat Yigit Can<sup>1</sup>, Ashley Proctor<sup>1</sup>, Sandeep Mannava<sup>3,5</sup>, Christoph  
5 Pröschel<sup>4</sup>, Whasil Lee<sup>1,2,3,5,\*</sup>

6 <sup>1</sup> Department of Biomedical Engineering, University of Rochester,

7 <sup>2</sup> Department of Pharmacology and Physiology, University of Rochester Medical Center,

8 <sup>3</sup> Center for Musculoskeletal Research, University of Rochester Medical Center,

9 <sup>4</sup> Department for Biomedical Genetics, University of Rochester,

10 <sup>5</sup> Department of Orthopaedics, University of Rochester Medical Center,

11 Rochester, NY 14620, USA

12 \* Address correspondence to: W. Lee, Department of Biomedical Engineering & Pharmacology and  
13 Physiology, University of Rochester; [wlee36@ur.rochester.edu](mailto:wlee36@ur.rochester.edu)

14 601 Elmwood Ave. Box 711 Rm 4.8553Rochester, NY14620, USA.

15

16 **Abstract**

17 **Objective:** The objective of this study is to understand the role of altered *in vivo* mechanical  
18 environments in knee joints post anterior cruciate ligament (ACL)-injury in chondrocyte vulnerability  
19 against mechanical stimuli and in the progression of post-traumatic osteoarthritis (PT-OA).

20 **Methods:** Differential *in vivo* mechanical environments were induced by unilateral ACL-injury (uni-ACL-I)  
21 and bilateral ACL-injury (bi-ACL-I) in 8-week-old female C57BL/6 mice. The gait parameters, the  
22 mechano-vulnerability of *in situ* chondrocytes, Young's moduli of cartilage extracellular matrix (ECM), and  
23 the histological assessment of OA severity (OARSI score) were compared between control and  
24 experimental groups at 0~8-weeks post-ACL-injury.

25 **Results:** We found that bi-ACL-I mice experience higher joint-loading on their both injured limbs, but uni-  
26 ACL-I mice balance their joint-loading between injured and uninjured hind limbs resulting in a reduced  
27 joint-loading during gait. We also found that at 4- and 8-week post-injury the higher weight-bearing hind  
28 limbs (i.e., bi-ACL-I) had the increased area of chondrocyte death induced by impact loading and higher  
29 OARSI score than the lower weight-bearing limbs (uni-ACL-I). Additionally, we found that at 8-weeks  
30 post-injury the ECM became stiffer in bi-ACL-I joints and softer in uni-ACL-I joints.

31 **Conclusions:** Our results show that ACL-injured limbs with lower *in vivo* joint-loading develops PT-OA  
32 significantly slower than injured limbs with higher joint-loading during gait. Our data also indicate that  
33 articular chondrocytes in severe PT-OA are more fragile from mechanical impacts than chondrocytes in  
34 healthy or mild PT-OA. Thus, preserving physiologic joint-loads on injured joints will reduce chondrocyte  
35 death post-injury and may delay PT-OA progression.

36

37 **Keywords**

38 Post-traumatic Osteoarthritis (PT-OA), anterior cruciate ligament (ACL)-injury, chondrocyte death,  
39 extracellular matrix (ECM), gait analysis

40 **Introduction**

41

42 Joint injury is a major risk factor of symptomatic osteoarthritis (OA), a prevalent and debilitating condition  
43 of load-bearing joints characterized by progressive degeneration of cartilage extracellular matrix (ECM)<sup>1-7</sup>.  
44 Anterior cruciate ligament (ACL)-tear is the most common knee injury and more than 50% of ACL-injury  
45 patients develop post-traumatic (PT)-OA within 5~20 years post-injury regardless of whether or not they  
46 have ACL-reconstruction surgery<sup>8-12</sup>. Unfortunately, the majority of injuries occur in young adults between  
47 the ages of 15 and 24<sup>13-17</sup>, and these young adults with ACL injuries are more likely to develop OA before  
48 the age of 40<sup>11, 18</sup>. Risk of ACL-revision surgery is especially pronounced in younger patients, who are  
49 subject to multiple revision surgeries over a lifetime, and who may have only options of surgical total knee  
50 joint replacement to treat PT-OA<sup>19, 20</sup>. The hallmark of ACL-injury is knee joint destabilization. ACL, a  
51 ligament directly connecting the femur to the tibia, stabilizes the knee joint in the anterior-to-posterior  
52 direction, prevents anterior-tibial subluxation, as well as provides rotational stability. A sudden turn or non-  
53 contact mechanism typically causes an ACL tear resulting in knee subluxation, pivot shift, and joint  
54 instability indicated in altered joint kinematics and gait patterns<sup>21-27</sup>.

55

56 Mechanical factors heavily influence chondrocyte' biosynthetic activities and ECM homeostasis, and  
57 chondrocyte mechanotransduction plays a critical role in the pathogenesis of OA<sup>6, 28-33</sup>. Thus, the abnormal  
58 mechanical loading is presumed to contribute to OA progression post-ACL-injury. In addition, ACL-injuries  
59 often lead to more severe OA progression due to the concomitant damages on the meniscus, other  
60 ligaments, or articular cartilage<sup>34-37</sup>. Furthermore, contralateral non-injured knee joints have high risks of  
61 joint injuries due to the compensatory aberrant joint loading<sup>38, 39</sup>, and 12% of ACL-injured patients have  
62 recurring ACL ruptures in their contralateral knees within 2 to 5 years post-injury<sup>40, 41</sup>. These combinations  
63 of damages may cause individuals to load different degrees of abnormal mechanical stimuli on their ACL-  
64 injured joints, thus may lead to diverse rates of PT-OA progression.

65

66 Several murine PT-OA studies have identified the increased chondrocyte death in injured cartilage by  
67 histological assessment<sup>42-44</sup>. Since promoting chondrocyte survival after joint injury may delay cartilage  
68 degradation<sup>45-49</sup>, it is important to understand how the abnormal *in vivo* mechanical loads alter chondrocyte  
69 viability and cartilage homeostasis post-injuries. In addition, the ability of chondrocytes to withstand  
70 injurious forces, termed 'mechano-vulnerability', depends on mechano-sensitivity of chondrocytes and  
71 mechanical properties of the ECM. Currently, a limited information is known about the effects of *in vivo*  
72 loading on chondrocyte viability post-injury, and loading-dependent chondrocyte mechano-vulnerability and  
73 the mechanical properties of ECM have not been studied over the PT-OA progression post-ACL-I.

74

75 Here, we investigate the extent to which alterations in *in-vivo* mechanical loading environments impact  
76 chondrocyte mechano-vulnerability in ACL-injured knees using a non-invasive ACL injury mouse model.  
77 The alterations in *in vivo* mechanical environment were induced through unilateral (uni-ACL-I) and bi-lateral  
78 (bi-ACL-I) ACL injuries of hind legs. We found that uni-ACL-I mice experienced lower weight-bearing in  
79 their hind paws during the gait as compared to bi-ACL-I mice. We also found that articular cartilage of ACL-  
80 injured mice with higher weight-bearing (i.e., bi-ACL-I) had more mechanically vulnerable chondrocytes and  
81 more severe cartilage degradation, the evidence of PT-OA, as compared to injured mice with lower gait-  
82 associated weight-bearing (i.e., uni-ACL-I). Our findings demonstrate that it is critical to avoid abnormal  
83 joint mechanics and reduce chondrocyte mechano-sensitivity post-ACL-I as a potential treatment aimed to  
84 delay or halt PT-OA progression.

85

## 86 **Methods**

### 87 **Non-invasive ACL injuries**

88 We examined female mice considering the relatively understudied PT-OA in females despite a higher risk  
89 of PT-OA<sup>50, 51</sup> and ACL-tear in females than males<sup>14, 52-54</sup>. PT-OA was induced by a non-invasive ACL-  
90 injury<sup>55</sup> in 8-10-week-old female C57BL/6 mice unilaterally (injury in one knee) or bilaterally (injuries in both  
91 knees). Briefly, mice were anesthetized and placed on a custom-built Styrofoam. A custom-built strain

92 gauge-instrumented probe (Fig. 1a-b) was placed onto the skin over the patellar tendon, and an axial force  
93 was manually applied to the distal femur along the axis of the femoral shaft. The temporal force profiles  
94 were recorded using an Arduino system. The average rupture force was  $14.2 \pm 0.3$  N and the loading rate  
95 was  $1.52 \pm 0.05$  N/s ( $n=94$  limbs) (Fig. 1c-e). Mice had positive Lachman tests and X-ray imaged were  
96 acquired immediately after the procedure to ensure that the injury had not caused a fracture of the tibia or  
97 femur. Mice were monitored for 3 days for signs of pain. This procedure was approved by the University of  
98 Rochester Committee on Animal Resources (UCAR). (see supplemental material for the detailed method).

99

## 100 **Gait analysis**

101 Alteration in mouse gait post-ACL-I was assessed by Noldus CatWalk XT automated gait analysis system  
102 (Noldus Information Technology, XT10.6)<sup>56, 57</sup>. Briefly, a mouse walked across an enclosed space on top  
103 of a 50 cm long glass plate illuminated by an internally reflected green LED light. Below the glass, a high-  
104 speed color camera captured green light refraction of the illuminated mouse paw prints when the paw  
105 touched the glass. Red light illuminated the top of the glass plate to capture mouse silhouette during the  
106 gait (Fig. 2a-b). Each mouse walked 3 compliant runs with a run variance below 65%. Gait analysis was  
107 performed longitudinally at 4- and 8-weeks post-injury ( $n = 6$ /group). The hindlimb maximum Contact Mean  
108 Intensity was measured from the captured timeframe with the most intense pixels of the paw prints during  
109 a mouse's gait cycle indicating max mouse weight-bearing. The max Contact Mean Intensity of left and  
110 right hind limbs in bi-ACL-I group were averaged and compared to other groups. The Base of Support, a  
111 vertical distance between the hind limbs during the gait, was also measured to quantify mouse posture (Fig.  
112 2e-f). The Stand mean, a contact duration of hind paws on the walkway glass, was compared between  
113 groups (Suppl. Fig. 1). There was no difference in average mouse weight or running speed between uni-  
114 ACL-I and bi-ACL-I mice (Fig. 2d, g).

115

## 116 **Mechano-vulnerability assay (Impact-induced chondrocyte LIVE/DEAD assay)**

117 We quantified the vulnerability of chondrocytes on the *lateral* femoral condyles by 1 mJ impact<sup>58</sup>. Briefly,  
118 distal femurs were dissected and stained with calcein-AM and Propidium Iodide (PI) (R37601, Invitrogen),  
119 positioned in our custom-built impact device (Fig. 3a), then subjected to a 1 mJ kinetic energy on the patello-  
120 femoral groove. Chondrocytes on the lateral femoral condyles were z-stack imaged by a confocal  
121 microscope (FV3000, Olympus, UPlanSApo 10X/0.40 NA dry) before and after the impact. After the impact,  
122 specimens were re-stained with PI, an indicator of injured/dead cells, and re-imaged. Chondrocytes that  
123 lost calcein-labeling and became PI-positive were considered to be injured/dead, and the area of injured  
124 cells was quantified using ImageJ. (see supplemental material for the detailed method).

125

### 126 **Mechanical properties of articular cartilage**

127 A confocal microscope-based inverse finite element method (iFEM)<sup>59</sup> was used to quantify the altered  
128 intrinsic stiffness (Young's Modulus) of the ECM at 8-weeks post-injury. In brief, distal femurs were stained  
129 with 5'-DTAF (Sigma-Aldrich) to label the cartilage ECM, and placed on a cover glass of a custom-built  
130 mechanical device above a confocal microscope (Olympus FV3000, LUCPLFLN 40X NA = 0.6) (Fig. 2a).  
131 Confocal z-stacks of lateral femoral condyles were obtained before (baseline) and 5 min after applying a  
132 static load of 0.1 N (0.31  $\mu\text{m}/\text{pixel}$  in xy-plane and 0.89  $\mu\text{m}/\text{slice}$  in z-plane). The acquired confocal z-stacks  
133 were used to obtain thickness ratios (i.e., compressive tissue stretch  $\lambda_z$ ), maps of the infinitesimal tissue  
134 strain ( $\varepsilon_z = 1 - \text{thickness ratio}$ ), and peak compressive strains (strains within 5  $\mu\text{m}$  from the peak  
135 compressive strain). The compression experiments were simulated in FEBio using 3D FEMs<sup>60</sup> to determine  
136 the Young's modulus of the femoral ECM in different experimental groups (see supplemental material for  
137 detailed methods).

138

### 139 **Histological evaluation**

140 After 4- and 8-weeks post- injury, mouse tibio-femoral joints were fixed in 10% formalin, decalcified, and  
141 embedded in paraffin. Sagittal sections (7  $\mu\text{m}$  thick) of medial knee joints were stained with Safranin-O/Fast  
142 Green (Saf-O/FG, Applied Biosciences), and imaged by Virtual Slide Microscope System (Olympus VS120,

143 40X dry). Osteoarthritis Histopathology Assessment System (OARSI) scores<sup>61</sup> of femur and tibia cartilage  
144 are assessed in a blind-manner.

145

## 146 **Statistical analyses**

147 Cell death areas and OARSI score) were compared between the experimental groups using a Two-way  
148 Analysis of Variance (ANOVA) with a post-hoc Tukey test. Max Contact Mean Intensity, Base of Support  
149 and mouse mass were compared across experimental groups using repeated measures Two-way ANOVA  
150 with a post-hoc Tukey test. Compressive strains and Young's moduli of ECM were compared using a One-  
151 way ANOVA with a post-hoc Tukey test. Statistical differences were detected at a significance level ( $\alpha$ ) of  
152 0.05.

153

## 154 **Results**

155

156 To investigate the role of *in vivo* loading in PT-OA development post-ACL-I, we compared gait parameters  
157 of hind limbs, mechano-vulnerability of articular chondrocytes *in situ*, mechanical properties of the ECM,  
158 and OARSI score in experimental groups: mice without injury (Group 1: uninjured controls), mice with  
159 bilateral ACL injury (Group 2: bi-ACL-I), and mice with a unilateral ACL injury, where the contralateral knee  
160 joints served as the unilateral uninjured controls (Group 3: uni-ACL-uninjured, Group 4: uni-ACL-I) at 0~8  
161 weeks post-injury (Fig. 1f-i).

162

### 163 **Bilaterally ACL-injured mice experience higher weight-bearing in their hindlimbs during the gait** 164 **than unilaterally ACL-injured mice**

165 We first found that the bi-ACL-I joints exhibit significantly increased hindlimb Max Contact Mean Intensity  
166 (related to mouse weight-bearing, arbitrary unit (a.u.)) during mouse locomotion as compared to uni-ACL-I  
167 mice and uninjured control group at both 4- and 8-week post-injury (Fig. 2a-b; week 4:  $102.4 \pm 1.98$  a.u. vs.

168 72.3±1.54 a.u., week 8: 88.3±3.72 a.u. vs. 70.8±1.67 a.u., mean±SEM). In contrast, uni-ACL-I joints exhibit  
169 an increased Contact Intensity as compared to the uninjured control group only at 4-week (93.7 ± 2.45 a.u.)  
170 but not at 8-week post-injury (73.5±1.16 a.u.). Interestingly, contralateral uni-ACL-uninjured joints exhibit  
171 similar levels of joint loading at both 4- and 8-week post-injury (Fig. 2a-b). Next, there were noticeable  
172 alterations in mouse posture during the gait in terms of the Base of Support, the vertical distance between  
173 mouse hind limbs. Bi-ACL injured mice had a narrower Base of Support as compared to uninjured control  
174 mice, while mice in the uni-ACL group had a Base of Support similar to the uninjured controls (Fig. 2c). The  
175 average duration of the mouse paw print (stand mean) was similar across all experimental groups and time-  
176 points (Supplemental materials). We note that the walking speed and bodyweight of bi-ACL-I and uni-ACL-  
177 I mice were similar for the entire course of the experiment (4- and 8-weeks post-injury) allowing for fair  
178 comparisons of the analyzed gait parameters; yet these uni-ACL- and bi-ACL-injured mice walked slower  
179 than uninjured control mice. These differential data of Contact Mean intensity and Base of Support reveal  
180 that the injured cartilage in bi-ACL-I joints experiences higher *in vivo* joint-loading and more significant  
181 mechanical instability during gait than injured cartilage in uni-ACL-I.

182

### 183 ***In situ* chondrocytes in bi-ACL-I joints are more vulnerable to impact loading than chondrocytes in** 184 **uni-ACL-I or uninjured joints**

185 Chondrocyte survival is implicated in the pathogenesis of PT-OA, and cell viability and metabolism under  
186 physiologic and pathophysiologic mechanical environments is crucial for cartilage remodeling and  
187 homeostasis. Therefore, we quantified areas of chondrocyte death in load-bearing cartilage on femoral  
188 condyles induced by application of injurious 1mJ impacts onto isolated cartilage-on-bone explants (Fig.  
189 3a)<sup>58</sup>. This assay examines the mechano-vulnerability of *in situ* chondrocytes in load-bearing femoral  
190 cartilage, and the quantified areas of dead cells are presumed to represent the resilience of load-bearing  
191 chondrocytes against injuries *in vivo*. Interestingly, we found that bi-ACL-I joints exhibit the largest areas of  
192 cell death induced by impact loading at both 4- and 8-weeks post-injury. This result indicates that  
193 chondrocytes in bi-ACL-I became significantly more mechano-vulnerable than chondrocytes in uni-ACL-I  
194 or uninjured cartilage (Fig. 3b-c). In contrast, areas of dead cells in femurs of uni-ACL-I were comparable



195 to contralateral uninjured joints (uni-ACL-uninjured) and uninjured controls (control group) at both 4- and 8-  
196 weeks post-injury (Fig. 3b-c). This result reveals that chondrocytes in uni-ACL-I maintained their mechano-  
197 vulnerability as uninjured chondrocytes. We also observed that, at 0-week (3-5 days) post-injury, areas of  
198 chondrocyte death were significantly elevated in both the uni- and bi-ACL-I groups as compared to  
199 uninjured controls. This significantly elevated mechano-vulnerability at 0-week is presumed to be driven by  
200 acute inflammation post-injury in synovial joints<sup>62, 63</sup> (Control:  $11707.8 \pm 1081.4 \mu\text{m}^2$ , bi-ACL-I :  $16312.1 \pm$   
201  $901.1 \mu\text{m}^2$ , uni-ACL-uninjured:  $13449.8 \pm 535.3 \mu\text{m}^2$ , uni-ACL-I:  $22106.4 \pm 679.7 \mu\text{m}^2$ ; Supplemental  
202 material). Taken together, these data reveal that articular chondrocytes in bi-ACL-I joints become more  
203 vulnerable from injurious mechanical loading as compared to the chondrocytes in uni-ACL-I or uninjured  
204 joints as developing PTOA (Fig. 3).

205

#### 206 **Mechanical property of ECM: soften in uni-ACL-I, stiffen in bi-ACL-I at 8-weeks post-injury**

207 We measured alterations in ECM Young's modulus and cartilage thickness of lateral condyles at 8-weeks  
208 post-injury (Fig. 4, Supplemental material). We found that articular cartilage of uni-ACL-I had reduced  
209 Young's moduli and increased peak compressive infinitesimal strains relative to contralateral uninjured  
210 limbs ( $3.6 \pm 0.3 \text{ MPa}$  vs.  $7.8 \pm 1.5 \text{ MPa}$ ;  $35.4 \pm 1.1 \%$  vs.  $26.6 \pm 2.5 \%$ ; Fig. 4d-e), indicating cartilage softening  
211 and the onset of PTOA only in the injured limb but not in intact contralateral limb post-ACL-I. Interestingly,  
212 Young's modulus of cartilage in bi-ACL-I joints was almost two-fold higher than that of uninjured controls  
213 ( $11.4 \pm 1.2 \text{ MPa}$  vs.  $6.1 \pm 0.7 \text{ MPa}$ ; Fig. 4e). Cartilage thickness of bi-ACL-I was significantly reduced as  
214 compared to uninjured controls ( $29.8 \pm 0.8 \mu\text{m}$  vs.  $34.5 \pm 1.1 \mu\text{m}$ ; Supplemental material), suggesting cartilage  
215 degradation and erosion. Though not significant, reduction in cartilage thickness was also observed in both  
216 uni-ACL injured and uni-ACL-uninjured limbs as compared to uninjured controls (Supplemental material).  
217 Taken together, ECM of articular cartilage in uni-ACL-I group was less stiff and the most compressed by a  
218 static load among the groups, whereas bi-ACL-I group exhibited the stiffest and least compressed cartilage.  
219 These differences in mechanical properties of the ECM suggest that *in vivo* chondrocytes may experience  
220 distinct mechanical stimuli post-injury in our experimental groups (bi-ACL-I, uni-ACL, and uninjured

221 controls), which lead to a feed-forward distinct cellular mechano-sensitivity and biosynthetic activities, which  
222 in turn alter structural and mechanical properties of the ECM along the PT-OA development.

223

#### 224 **Bi-ACL-I joints develop more severe PT-OA than uni-ACL-I joints.**

225 Histological sections of the medial knee joints revealed that uni-ACL-I and bi-ACL-I induce different degrees  
226 of cartilage degeneration at 4- and 8-weeks post-injury (Fig.1f-g). Specifically, in the majority of bi-ACL-I  
227 joints, we observed an anterior shift of mouse tibias and menisci relative to the femurs. In addition,  
228 significant articular cartilage degradation occurred on the posterior side of the tibia in bi-ACL-I. In contrast,  
229 the majority of uni-ACL-I knees did not have meniscus shift, cartilage degradation on the posterior side of  
230 the tibia was less severe than in bi-ACL-I group, and tissue calcification was observed (Fig. 1g, \* marked  
231 region). The mean OARSI scores of cartilage on medial femoral condyles were 0.6 and 0.5 in uninjured  
232 control, 3.4 and 3.8 in bi-ACL-I, 2.3 and 1.2 in uni-ACL-I, and 0.6 and 0.5 in uni-ACL-uninjured at 4- and 8-  
233 weeks post-injury, respectively (Fig. 1h-i). The mean scores within the medial tibial plateau (MTP) were 0.2  
234 and 0.4 in uninjured controls, 4.2 and 4.7 in bi-ACL-I, 1.9 and 1.9 in uni-ACL-I, and 0.2 and 0.1 in uni-ACL-  
235 uninjured at 4- and 8-weeks post-injury, respectively (Fig.1h-i). These results suggest that mice with bi-  
236 ACL-I develop more severe or rapid PT-OA as compared to uni-ACL injured mice.

237

#### 238 **Discussion**

239 Joint injury is a risk factor for OA, and altered joint kinematics due to joint injury has been suggested to  
240 contribute to PT-OA development, whether by directly damaging chondrocytes and ECM or indirectly  
241 altering chondrocyte metabolism and ECM stiffness progressively. Understanding of cartilage  
242 mechanotransduction may shed the light into developing effective therapeutic strategies to treat PT-OA<sup>6</sup>  
243 <sup>64-68</sup>. Here, we made a step towards understanding the relationship between the *in vivo* joint loading and  
244 chondrocyte mechano-vulnerability in murine articular cartilage post unilateral or bilateral ACL-I. Our data  
245 revealed that a higher *in vivo* joint loading leads to more severe or more rapid PT-OA development post-  
246 ACL-I. Interestingly, articular chondrocytes in the more loaded femoral cartilage (i.e., in bi-ACL-I group)

247 were more mechano-vulnerable and more prone to cellular death by mechanical stimuli as compared to  
248 chondrocytes in the less loaded cartilage (i.e., in uni-ACL-I or uninjured control groups). Our findings  
249 suggest that it is critical to avoid abnormal joint mechanics and to tightly tune the chondrocyte  
250 mechanosensitivity post-ACL-I in order to slow down PT-OA progression.

251

252 Unilateral and bilateral ACL-I differentially altered mouse gait patterns. We found that weight-bearing in  
253 hind limbs of bi-ACL-I mice was higher than in uni-ACL-I limbs and in uninjured control limbs, while the  
254 walking speed and body weight were comparable between bi-ACL-I and uni-ACL-I mice at both 4- and 8-  
255 weeks post-injury. Since uni-ACL-I destabilizes one hindlimb knee joint and the contralateral joint stays  
256 intact, we anticipated that uni-ACL-I mice exhibit asymmetrical gait distribution with lower load-bearing on  
257 injured limbs. Contrary to our expectations and consistent with previous reports indicating that mice can  
258 restore a symmetric distribution of weight-bearing within 2-3 weeks following traumatic injury<sup>62, 69</sup>, uni-ACL-  
259 I mice compensated the unbalanced joints, and exhibited similar levels of weight-bearing in injured and  
260 contralateral uninjured hind limbs at 4- and 8- weeks post-injury. Another distinctive difference between uni-  
261 ACL-I and bi-ACL-I mice was in the Base of Support, the width of hind-limb positions during the mouse  
262 locomotion. We observed a significantly reduced Base of Support in bi-ACL-I mice at 4-, and 8-weeks post-  
263 injury, while uni-ACL-I mice showed a comparable length of the Base of Support with uninjured control  
264 mice. These data indicate that unilateral and bilateral ACL-I cause differential mechanical environments in  
265 injured limbs that can contribute to different degrees of PT-OA development, and allows to examine the  
266 effect of joint mechanics on cellular and tissue health.

267

268 Distinct cellular mechano-vulnerability was observed in articular chondrocytes in lateral femoral condyles  
269 of uninjured, uni-ACL-I and bi-ACL-I joints over PT-OA development. Since chondrocyte death precedes  
270 cartilage degeneration in OA, and thus by promoting chondrocyte survival post-injury would delay PT-OA  
271 pathogenesis, we examined the *in situ* chondrocyte survival due to the applied mechanical impacts post-  
272 ACL-I. At 0-week post-injury, we observed increased areas of chondrocyte death induced by 1mJ  
273 mechanical impacts in ACL-I joints (uni- and bi-ACL-I) as compared to the areas observed in uninjured

274 joints (Supplemental material). This increased mechano-vulnerability of chondrocytes in uni-ACL-I and bi-  
275 ACL-I groups is presumably due to the local acute inflammation as the early response of synovial joints to  
276 trauma<sup>62, 70</sup>. Interestingly, at both 4- and 8-weeks post-injury, articular chondrocytes in femoral condyles of  
277 bi-ACL-I joints were the most vulnerable to mechanical impacts than chondrocytes in the uninjured control  
278 group (Fig. 3). The vulnerability of articular chondrocytes in uni-ACL-I joints were comparable to the  
279 chondrocytes' vulnerability in contralateral uninjured joints or to uninjured control limbs at 4- and 8-week  
280 post-injury. Importantly, these trends in cell mechano-vulnerability are similar to the trends of hindlimb  
281 weight bearing observed during mouse locomotion. We also observed that baseline cell death (cell death  
282 before the application of mechanical impacts) was elevated on medial femoral condyles as compared to  
283 cell death on lateral condyles, which is consistent with a study conducted by Berke et al.<sup>62</sup>. Therefore, we  
284 anticipate that medial cartilage endures higher degrees of abnormal mechanical loads post-ACL-I than  
285 lateral cartilage does, thereby causing more rapid cartilage degradation by altering chondrocyte mechano-  
286 sensitivity and cartilage integrity.

287

288 Distinct mechanical properties of cartilage ECM were also observed in lateral femoral condyles of uni-ACL-  
289 I and bi-ACL-I joints at 8-weeks post-injury. Based on the equilibrium Young's moduli, uni-ACL-I limbs have  
290 significantly lower ECM modulus as compared to ECM in contralateral uninjured or control uninjured limbs  
291 at 8-weeks post-injury. This reduction in ECM modulus corresponded to moderate PT-OA levels with 2~4  
292 OARSI scores (Fig. 1g-i). However, and to our surprise, bi-ACL-I knee joints showed a significantly  
293 increased Young's moduli of femoral articular cartilage and the most severe OARSI scores than other  
294 experimental groups (Fig. 1g-i). Altered cartilage moduli indicate OA progression and cartilage erosion in  
295 PT-OA<sup>71-74</sup>. Doyran et al. has reported a similar transition of cartilage stiffness over PT-OA development in  
296 a murine destabilized medial meniscus (DMM) model<sup>71</sup>. In their animal model, the ECM of medial condyles  
297 of injured limbs had decreased nanoindentation modulus as compared to the ECM of sham-surgery limbs  
298 at 1~8-weeks post-DMM-injury, then the modulus recovered significantly at 12-weeks post-injury when OA  
299 was the most severe based on their histological analysis<sup>71</sup>. Articular cartilage has a depth-dependent  
300 gradient in its compressive modulus with the less stiff superficial cartilage layer and the stiffer cartilage in

301 deeper layers reaching the bone<sup>75, 76</sup>. Cartilage thickness of femoral condyles was reduced in both uni-ACL-  
302 I and bi-ACL-I, yet bi-ACL-I showed slightly more reduced cartilage thickness and higher radius of curvature  
303 than uni-ACL-I. We speculate that the stiffening of the ECM in bi-ACL-I was due to the more severe  
304 degradation of the superficial cartilage layer than in uni-ACL-I joints. Taking together, our ECM modulus  
305 and histology data indicate that bi-ACL-I joints have more severe OA than uni-ACL-I joints, and cartilage of  
306 bi-ACL-I is stiffer than cartilage of uni-ACL-I. Ironically, despite stiffened ECM, articular chondrocytes in bi-  
307 ACL-I were more sensitive to mechanical impacts at 4- and 8-weeks post-injury. Stiffened ECM did not  
308 lessen the effect of mechanical impacts on *in situ* chondrocytes, but increased impact-induced chondrocyte  
309 death in bi-ACL-I joints. These data suggest that chondrocytes in bi-ACL-I were more fragile and impaired  
310 more upon mechanical stimuli.

311

312 Considering the crucial role of chondrocyte viability in cartilage homeostasis, our results suggest that the  
313 increased mechano-vulnerability of chondrocytes contributes to an accelerated PT-OA pathogenesis. Thus,  
314 we anticipate the homeostasis of cellular mechano-sensitivity, or mechanical-injury-sensitivity, is critical to  
315 delay PT-OA. A group of mechanosensing and mechanotransducing molecules may be regulated over PT-  
316 OA development and tune cellular mechano-sensitivity under abnormal joint mechanics and inflammation  
317 post-ACL-I. For instance, dysregulated integrin  $\alpha_v\beta_3$  and their associated ligands may play essential roles  
318 in disrupting chondrocyte-ECM interactions over OA progression<sup>77-79</sup>, as well as Piezo1 may be augmented  
319 via IL-1-mediated inflammatory patho-mechanisms<sup>80, 81</sup>. Future research will investigate the chondrocyte  
320 mechano-vulnerability based on mechanosensors and mechanotransducers and their local ECM properties  
321 over PT-OA development.

322

### 323 **Conclusion**

324 In this study, we quantified chondrocyte vulnerability and ECM mechanics on articular cartilage in load-  
325 bearing knee femoral joints over OA development post ACL-injury. We found the *in vivo* joint loading-  
326 dependent changes on chondrocytes' mechano-vulnerability over the PT-OA development in female mice

327 post-ACL-I. To our knowledge, this is the first study comparing the mechano-vulnerability of chondrocytes  
328 and the mechanical properties of ECM between unilateral and bilateral ACL-injuries in female mice. Our  
329 data reveal that unilateral ACL-I mice compensate and balance their joint loading between injured and  
330 uninjured hind limbs, resulting in the delayed progression of PT-OA with minimal changes on cellular  
331 mechano-vulnerability as compared to injured knees of bilateral ACL-I mice. This study suggests that the  
332 reduction in knee joint loading may delay ACL injury-associated progression of OA. Furthermore, patients  
333 with injuries in both of their joints may have a higher risk to develop PT-OA than the patients who do not  
334 have another joint injury in their contralateral knees because of the increased joint-loading. Our results  
335 support therapeutic interventions to tune cellular mechano-sensitivity and physical therapy to correct  
336 aberrant joint loading in ACL-injured legs to slow down PT-OA progression.

337

#### 338 **Additional materials and methods**

339 Additional materials and methods are provided in Supplementary files.

340

#### 341 **Author contributions**

342 WL & SM conceived and designed the study. AK, AE, NYC and AP performed experiments. AK, AE, NYC,  
343 CP and WL analyzed and interpreted the data. AK, AE, NYC, SM, CP and WL were involved in drafting the  
344 manuscript for important intellectual content and all authors approved the final version of the manuscript.

345

#### 346 **Conflict of interest**

347 The authors declare that they have no conflict of interest.

348

#### 349 **Role of funding source**

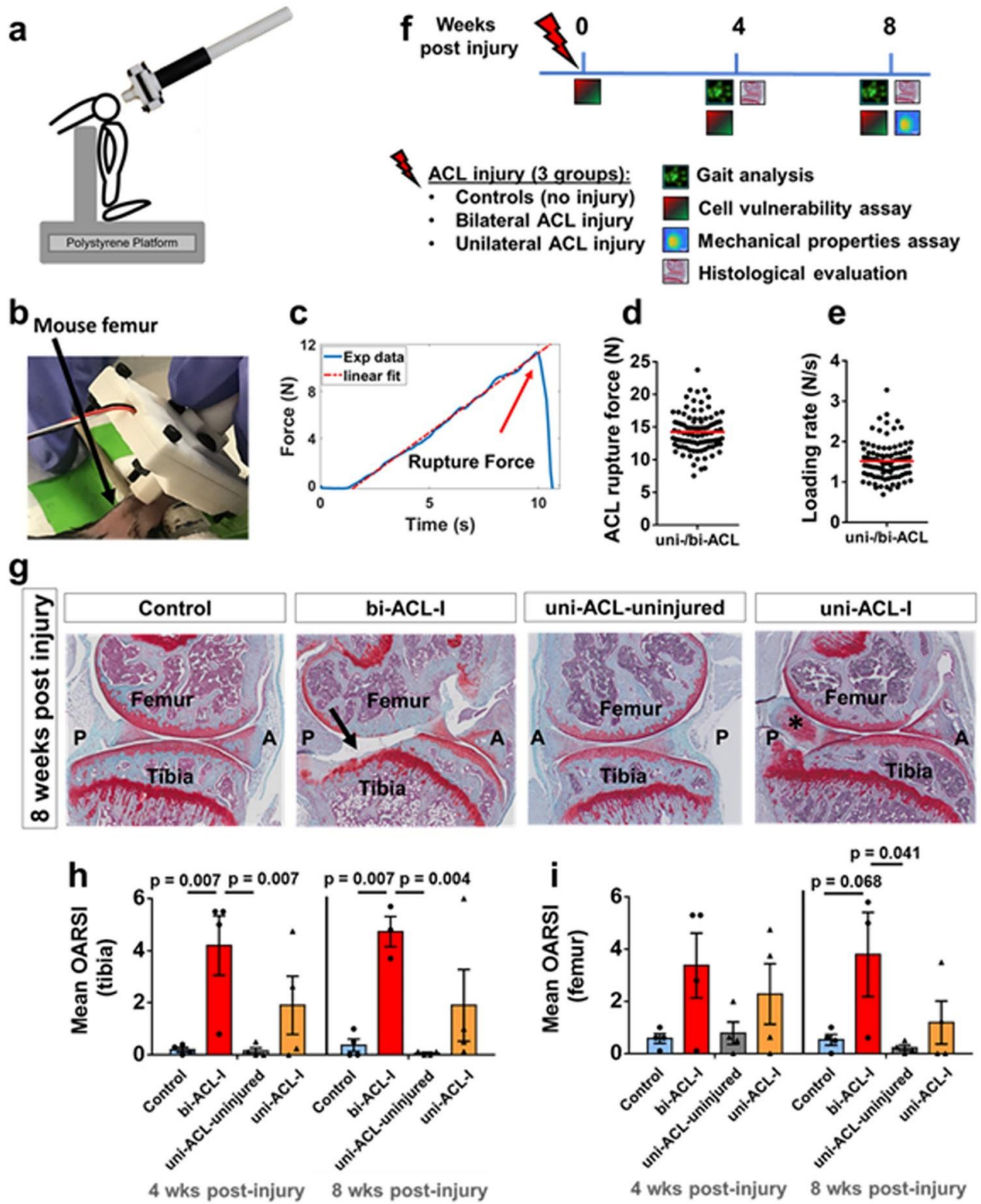
350 This work was supported in part by funds from the National Institute of Arthritis and Musculoskeletal and  
351 Skin Diseases (NIAMS) under award numbers P30 AR069655 and T32 AR076950. The content is solely  
352 the responsibility of the authors and does not necessarily represent the official views of the National  
353 Institutes of Health.

354

355 **Acknowledgements**

356 The authors thank Dr. Robert Dirksen for continuous research discussion. We also thank Center for  
357 Musculoskeletal Research (CMSR) Histology Core and University of Rochester Committee on Animal  
358 Resources (UCAR) for their technical assistance.

359 **Figure**



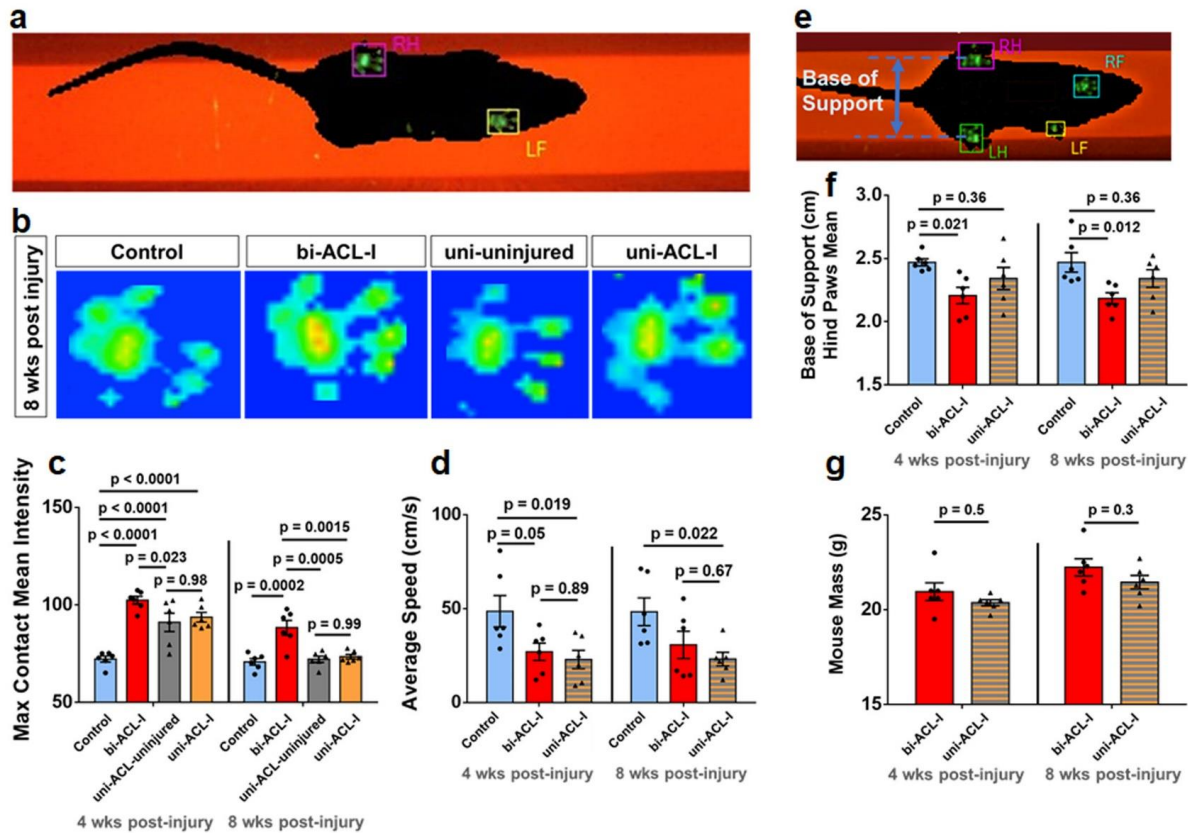
360

361 **Fig 1. Non-invasive ACL-injury method and study design.**



362 (a) Schematic representation and (b) a representative figure of the experimental setup where the ACL  
363 injuries were induced with a custom-built strain gauge-instrumented device by applying axial force along  
364 the femoral shaft until a distinct sound of ACL tear was heard and the force drop was felt. The method was  
365 adapted from [Zhang 2020]. (c) Representative force-time curve obtained during the ACL injury procedure.  
366 The rupture force is indicated by the arrow, and the dashed line indicates linear curve fit from which the  
367 loading rate was calculated. (d, e) Quantification of ACL rupture force and loading rate. Each data point  
368 represents ACL injured limb and red line denotes the mean of the data. (f) Study design. ACL injuries were  
369 performed on either one knee joint (uni-ACL-I group), or on both knee joints (bi-ACL-I group) in 8-9-week-  
370 old female C57BL/6 mice. Gait, cell vulnerability, mechanical properties, and histological analysis were  
371 assessed at different timepoints post ACL injury. (g-i) Histological evaluation of articular cartilage in murine  
372 knee joints in 3 experimental groups (Control, bi-ACL-I, uni-ACL: injured and contralateral uninjured) at 4-,  
373 and 8- weeks post ACL-I timepoints. (g) Representative SaFO/FG-stained sagittal histological sections of  
374 medial side of mouse knee joints in control, bi-ACL-I, uni-ACL-I, and the contralateral uni-ACL-uninjured 8  
375 weeks post ACL injury. Significant articular cartilage degradation (arrow) is evident on the bi-ACL injured  
376 knee, indicative of PTOA. Tissue calcification (\*) was also observed on the uni-ACL-injured knees. A and  
377 P denote anterior and posterior direction of a knee joint. (h, i) Semiquantitative assessment of cartilage  
378 degradation on mouse (h) proximal tibias and (i) distal femurs using OARSI scoring system (n = 3-4  
379 mice/group). Each data point represents an average of blinded scoring by 4 individuals. Higher OARSI  
380 scores (max = 6) indicate a higher degree of cartilage degradation. OARSI scores were compared using a  
381 Two-way ANOVA with a post-hoc Tukey test. Data are mean  $\pm$  SEM.  $p \leq 0.05$  indicates statistical difference  
382 between the groups.

383



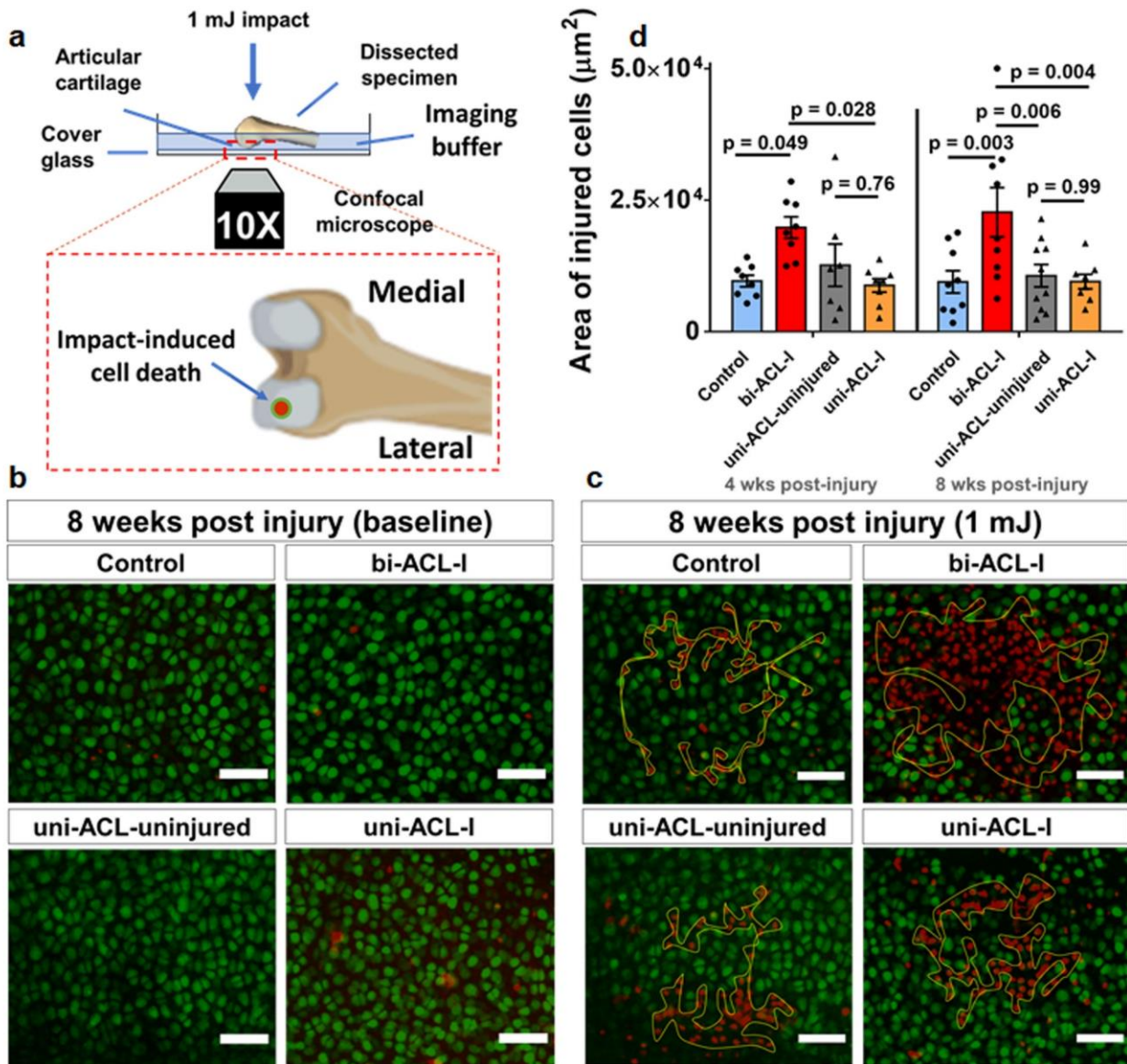
384

385 **Fig 2. Bi-ACL-I and uni-ACL-I exhibit distinct weight bearing during locomotion.**

386 (a) Representative snapshot of intensity of mouse paw-prints on illuminated platform of a Noldus CatWalk  
 387 XT system during gait analysis. (b) Representative snapshots of hind paw-print intensities at 8-weeks post-  
 388 injury in different experimental groups. See supplemental videos of representative 3D contact intensity plots  
 389 during mouse locomotion. (c) Quantification of maximum contact mean intensity in experimental and control  
 390 groups. Note that in bi-ACL-I and uninjured control mice max contact mean intensities were averaged for  
 391 both hind limbs per mouse, while uni-ACL-I and uni-ACL-uninjured hindlimbs were treated separately. (d)  
 392 Average mouse speed in 3 experimental groups (Control, bi-ACL-I, uni-ACL-I) at 4- and 8-weeks post-ACL-  
 393 I. (e) Representative micrograph of a mouse on a CatWalk platform with the indicated base of support as  
 394 the width between mouse hindlimbs during locomotion, and (f) quantification of mean base of support. (g)  
 395 Measurement of mouse mass in bi-ACL-I and uni-ACL-I groups prior to gait analysis at 4- and 8-weeks  
 396 post-injury. 6 mice per group were used to longitudinally assess their gait. Contact intensities, average  
 397 speeds, base of support, and mouse mass were compared using repeated measures Two-way ANOVA

398 with a post-hoc Tukey test. Data are mean  $\pm$  SEM.  $p < 0.05$  indicates statistical difference between the  
 399 groups.

400



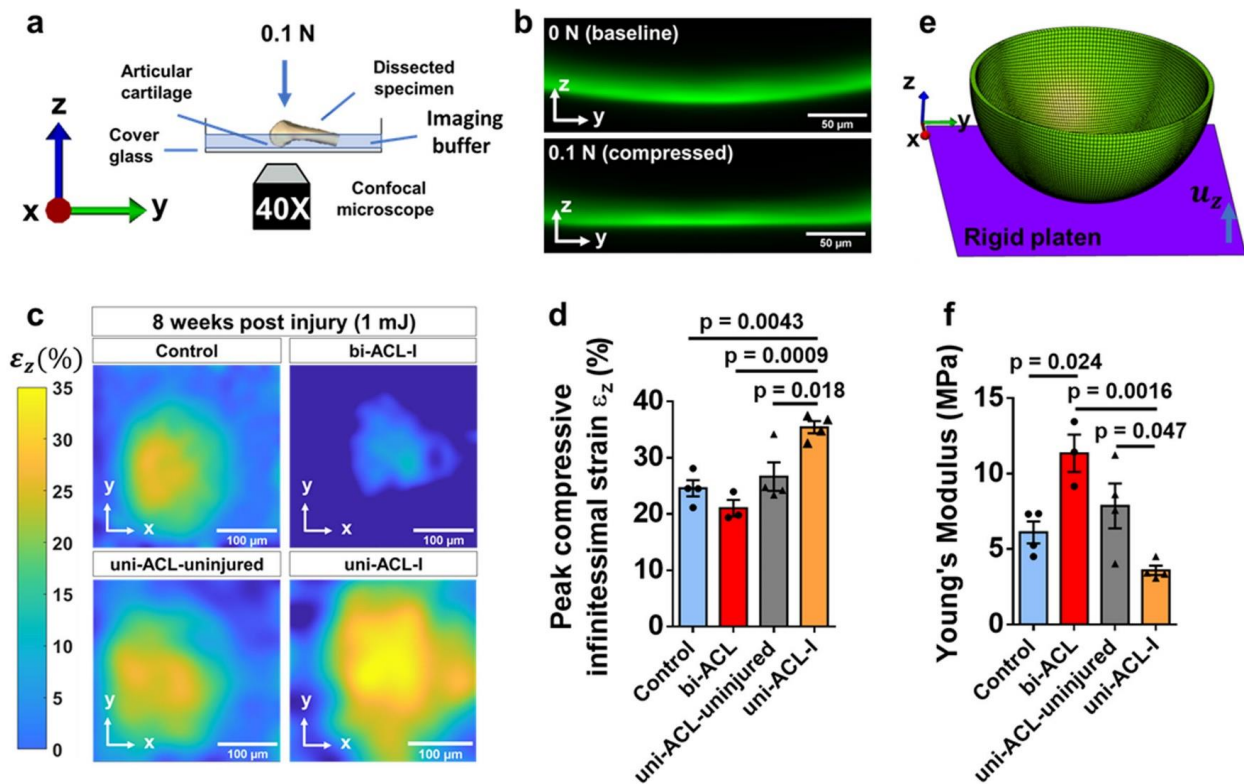
401

402 **Fig. 3 Chondrocytes in bi-ACL-I mice are more vulnerable than in uni-ACL-I mice.**

403 (a) Schematic representation of mechano-vulnerability experimental setup. Vitrally stained *in situ*  
 404 chondrocytes on lateral condyles of harvested distal femurs were imaged before and after the application  
 405 of 1 mJ kinetic energy impacts. A zoomed-in inset shows a view of femoral condyles in the imaging plane

406 where an impact-induced cell death is analyzed on the lateral condyles. **(b, c)** Representative z-projections  
 407 of confocal micrographs of live/dead (green/red) chondrocytes acquired **(b)** before and **(c)** after the impact  
 408 at 8 weeks post injury. Yellow contours in **(c)** indicate areas of injured/dead cells due to the applied 1mJ  
 409 impact. The scale bars are 50  $\mu$ m. **(d)** Quantification of impact-induced areas (within yellow contours) of  
 410 injured cells on surface of lateral femoral condyles in the experimental groups at 4- and 8-weeks post ACL-  
 411 I time-points (n = 6-9 limbs/group). The areas were compared using a Two-way ANOVA with a post-hoc  
 412 Tukey test. Data are mean  $\pm$  SEM.  $p < 0.05$  indicates statistical difference between the groups.

413



414

415 **Fig. 4 The ECM of Femoral lateral condyles in bi-ACL-I hindlimbs are stiffer than the ECM in uni-**  
 416 **ACL-I hind limbs.**

417 (a) Schematic representation of experimental setup to assess compressive strain and mechanical  
 418 properties of cartilage ECM on lateral femoral condyles. (b) Representative confocal micrographs of  
 419 fluorescently stained cartilage on the lateral femoral condyle (top) before and (bottom) during cartilage

420 compression after the specimens were subjected to a 0.1 N static loading for 5 min. Scale bar is 50 mm.  
421 (c) Representative maps of compressive strain of cartilage ECM on lateral femoral condyles of dissected  
422 specimens subjected to a 0.1 N static loading for 5 min in 3 experimental groups (Control, bi-ACL-I, uni-  
423 ACL: injured and contralateral uninjured) at 8-weeks post ACL-I time-point ( $n = 3-4$  mice/group). Scale bar  
424 is 100  $\mu$ m. (d) Quantification of the peak compressive infinitesimal strain in the experimental groups. (e)  
425 Representative 3D geometry of cartilage FEM to simulate the compression experiment and quantify ECM  
426 Young's modulus via an inverse FE analysis. The cartilage is compressed with a rigid plate with prescribed  
427 experimentally measured boundary displacements ( $u_z$ ). (f) Quantification of solid matrix Young's modulus  
428 of cartilage on lateral femoral condyles in the experimental groups using a finite element-based method  
429 and parameters including reaction force, boundary displacement, and cartilage geometry (see  
430 Supplementary materials). Compressive strains and Young's moduli were compared using a One-way  
431 ANOVA with a post-hoc Tukey test. Data are mean  $\pm$  SEM.  $p \leq 0.05$  indicates statistical difference between  
432 the groups.

433

#### 434 **Reference**

- 435 1. Van Spil WE, Kubassova O, Boesen M, Bay-Jensen AC, Mobasheri A. Osteoarthritis phenotypes  
436 and novel therapeutic targets. *Biochem Pharmacol* 2019; 165: 41-48.
- 437 2. Devezza LA, Loeser RF. Is osteoarthritis one disease or a collection of many? *Rheumatology*  
438 (Oxford) 2018; 57: iv34-iv42.
- 439 3. Karsdal MA, Michaelis M, Ladel C, Siebuhr AS, Bihlet AR, Andersen JR, et al. Disease-modifying  
440 treatments for osteoarthritis (DMOADs) of the knee and hip: lessons learned from failures and  
441 opportunities for the future. *Osteoarthritis Cartilage* 2016; 24: 2013-2021.
- 442 4. Akkiraju H, Nohe A. Role of Chondrocytes in Cartilage Formation, Progression of Osteoarthritis  
443 and Cartilage Regeneration. *J Dev Biol* 2015; 3: 177-192.
- 444 5. Cruz-Almeida Y, Sibille KT, Goodin BR, Petrov ME, Bartley EJ, Riley JL, 3rd, et al. Racial and  
445 ethnic differences in older adults with knee osteoarthritis. *Arthritis Rheumatol* 2014; 66: 1800-  
446 1810.

- 447 6. Guilak F. Biomechanical factors in osteoarthritis. *Best Pract Res Clin Rheumatol* 2011; 25: 815-  
448 823.
- 449 7. Zhang Y, Jordan JM. Epidemiology of osteoarthritis. *Clin Geriatr Med* 2010; 26: 355-369.
- 450 8. Carbone A, Rodeo S. Review of current understanding of post-traumatic osteoarthritis resulting  
451 from sports injuries. *J Orthop Res* 2017; 35: 397-405.
- 452 9. Whittaker JL, Woodhouse LJ, Nettel-Aguirre A, Emery CA. Outcomes associated with early post-  
453 traumatic osteoarthritis and other negative health consequences 3-10 years following knee joint  
454 injury in youth sport. *Osteoarthritis Cartilage* 2015; 23: 1122-1129.
- 455 10. Racine J, Aaron RK. Post-traumatic osteoarthritis after ACL injury. *R I Med J (2013) 2014*; 97: 25-  
456 28.
- 457 11. Lohmander LS, Englund PM, Dahl LL, Roos EM. The long-term consequence of anterior cruciate  
458 ligament and meniscus injuries: osteoarthritis. *Am J Sports Med* 2007; 35: 1756-1769.
- 459 12. Roos EM. Joint injury causes knee osteoarthritis in young adults. *Curr Opin Rheumatol* 2005; 17:  
460 195-200.
- 461 13. Beck NA, Lawrence JTR, Nordin JD, Defor TA, Tompkins M. ACL Tears in School-Aged Children  
462 and Adolescents Over 20 Years. *Pediatrics* 2017; 139.
- 463 14. Gornitzky AL, Lott A, Yellin JL, Fabricant PD, Lawrence JT, Ganley TJ. Sport-Specific Yearly Risk  
464 and Incidence of Anterior Cruciate Ligament Tears in High School Athletes: A Systematic Review  
465 and Meta-analysis. *Am J Sports Med* 2016; 44: 2716-2723.
- 466 15. Sanders TL, Maradit Kremers H, Bryan AJ, Larson DR, Dahm DL, Levy BA, et al. Incidence of  
467 Anterior Cruciate Ligament Tears and Reconstruction: A 21-Year Population-Based Study. *Am J*  
468 *Sports Med* 2016; 44: 1502-1507.
- 469 16. Gage BE, McIlvain NM, Collins CL, Fields SK, Comstock RD. Epidemiology of 6.6 million knee  
470 injuries presenting to United States emergency departments from 1999 through 2008. *Acad*  
471 *Emerg Med* 2012; 19: 378-385.
- 472 17. Moses B, Orchard J, Orchard J. Systematic review: Annual incidence of ACL injury and surgery in  
473 various populations. *Res Sports Med* 2012; 20: 157-179.

- 474 18. Oiestad BE, Holm I, Aune AK, Gunderson R, Myklebust G, Engebretsen L, et al. Knee function  
475 and prevalence of knee osteoarthritis after anterior cruciate ligament reconstruction: a  
476 prospective study with 10 to 15 years of follow-up. *Am J Sports Med* 2010; 38: 2201-2210.
- 477 19. Bhandari M, Smith J, Miller LE, Block JE. Clinical and economic burden of revision knee  
478 arthroplasty. *Clin Med Insights Arthritis Musculoskelet Disord* 2012; 5: 89-94.
- 479 20. Khan T, Alvand A, Prieto-Alhambra D, Culliford DJ, Judge A, Jackson WF, et al. ACL and  
480 meniscal injuries increase the risk of primary total knee replacement for osteoarthritis: a matched  
481 case-control study using the Clinical Practice Research Datalink (CPRD). *Br J Sports Med* 2018.
- 482 21. Zheng T, Song GY, Feng H, Zhang H, Li Y, Li X, et al. Lateral Meniscus Posterior Root Lesion  
483 Influences Anterior Tibial Subluxation of the Lateral Compartment in Extension After Anterior  
484 Cruciate Ligament Injury. *Am J Sports Med* 2020; 48: 838-846.
- 485 22. Wellsandt E, Khandha A, Capin J, Buchanan TS, Snyder-Mackler L. Operative and nonoperative  
486 management of anterior cruciate ligament injury: Differences in gait biomechanics at 5 years.  
487 *Journal of Orthopaedic Research* 2020; 38: 2675-2684.
- 488 23. Minami T, Muneta T, Sekiya I, Watanabe T, Mochizuki T, Horie M, et al. Lateral meniscus  
489 posterior root tear contributes to anterolateral rotational instability and meniscus extrusion in  
490 anterior cruciate ligament-injured patients. *Knee Surg Sports Traumatol Arthrosc* 2018; 26: 1174-  
491 1181.
- 492 24. Gardinier ES, Manal K, Buchanan TS, Snyder-Mackler L. Altered loading in the injured knee after  
493 ACL rupture. *J Orthop Res* 2013; 31: 458-464.
- 494 25. Brody JM, Lin HM, Hulstyn MJ, Tung GA. Lateral meniscus root tear and meniscus extrusion with  
495 anterior cruciate ligament tear. *Radiology* 2006; 239: 805-810.
- 496 26. Georgoulis AD, Papadonikolakis A, Papageorgiou CD, Mitsou A, Stergiou N. Three-dimensional  
497 tibiofemoral kinematics of the anterior cruciate ligament-deficient and reconstructed knee during  
498 walking. *Am J Sports Med* 2003; 31: 75-79.
- 499 27. Rudolph KS, Eastlack ME, Axe MJ, Snyder-Mackler L. 1998 Basmajian Student Award Paper:  
500 Movement patterns after anterior cruciate ligament injury: a comparison of patients who

- 501           compensate well for the injury and those who require operative stabilization. *J Electromyogr*  
502           *Kinesiol* 1998; 8: 349-362.
- 503   28.   Sanchez-Adams J, Leddy HA, McNulty AL, O'Connor CJ, Guilak F. The mechanobiology of  
504           articular cartilage: bearing the burden of osteoarthritis. *Curr Rheumatol Rep* 2014; 16: 451.
- 505   29.   Griffin TM, Guilak F. The role of mechanical loading in the onset and progression of osteoarthritis.  
506           *Exerc Sport Sci Rev* 2005; 33: 195-200.
- 507   30.   Anderson DD, Chubinskaya S, Guilak F, Martin JA, Oegema TR, Olson SA, et al. Post-traumatic  
508           osteoarthritis: improved understanding and opportunities for early intervention. *J Orthop Res*  
509           2011; 29: 802-809.
- 510   31.   Diekman BO, Wu CL, Louer CR, Furman BD, Huebner JL, Kraus VB, et al. Intra-articular delivery  
511           of purified mesenchymal stem cells from C57BL/6 or MRL/MpJ superhealer mice prevents post-  
512           traumatic arthritis. *Cell Transplant* 2012.
- 513   32.   Mangiapani DS, Zeitler E, Furman BD, Huebner JL, Kraus VB, Guilak F, et al. Inhibition of  
514           Interleukin-1 prevents post-traumatic arthritis following articular fracture of the mouse knee.  
515           *Transactions of the Orthopaedic Research Society*, vol. 362012:711.
- 516   33.   Chubinskaya S, Haudenschild D, Gasser S, Stannard J, Krettek C, Borrelli J, Jr. Articular  
517           Cartilage Injury and Potential Remedies. *J Orthop Trauma* 2015; 29 Suppl 12: S47-52.
- 518   34.   Ahn JH, Lee YS, Yoo JC, Chang MJ, Park SJ, Pae YR. Results of Arthroscopic All-Inside Repair  
519           for Lateral Meniscus Root Tear in Patients Undergoing Concomitant Anterior Cruciate Ligament  
520           Reconstruction. *Arthroscopy-the Journal of Arthroscopic and Related Surgery* 2010; 26: 67-75.
- 521   35.   Yoon KH, Yoo JH, Kim KI. Bone contusion and associated meniscal and medial collateral  
522           ligament injury in patients with anterior cruciate ligament rupture. *J Bone Joint Surg Am* 2011; 93:  
523           1510-1518.
- 524   36.   Clancy WG, Jr., Sutherland TB. Combined posterior cruciate ligament injuries. *Clin Sports Med*  
525           1994; 13: 629-647.
- 526   37.   Maffulli N, Binfield PM, King JB. Articular cartilage lesions in the symptomatic anterior cruciate  
527           ligament-deficient knee. *Arthroscopy* 2003; 19: 685-690.



- 528 38. Berchuck M, Andriacchi TP, Bach BR, Reider B. Gait adaptations by patients who have a  
529 deficient anterior cruciate ligament. *J Bone Joint Surg Am* 1990; 72: 871-877.
- 530 39. Hurd WJ, Snyder-Mackler L. Knee instability after acute ACL rupture affects movement patterns  
531 during the mid-stance phase of gait. *J Orthop Res* 2007; 25: 1369-1377.
- 532 40. Wright RW, Dunn WR, Amendola A, Andrish JT, Bergfeld J, Kaeding CC, et al. Risk of tearing the  
533 intact anterior cruciate ligament in the contralateral knee and rupturing the anterior cruciate  
534 ligament graft during the first 2 years after anterior cruciate ligament reconstruction: a prospective  
535 MOON cohort study. *Am J Sports Med* 2007; 35: 1131-1134.
- 536 41. Wright RW, Magnussen RA, Dunn WR, Spindler KP. Ipsilateral graft and contralateral ACL  
537 rupture at five years or more following ACL reconstruction: a systematic review. *J Bone Joint*  
538 *Surg Am* 2011; 93: 1159-1165.
- 539 42. David MA, Smith MK, Pilachowski RN, White AT, Locke RC, Price C. Early, focal changes in  
540 cartilage cellularity and structure following surgically induced meniscal destabilization in the  
541 mouse. *Journal of Orthopaedic Research* 2017; 35: 537-547.
- 542 43. McNulty MA, Loeser RF, Davey C, Callahan MF, Ferguson CM, Carlson CS. Histopathology of  
543 naturally occurring and surgically induced osteoarthritis in mice. *Osteoarthritis Cartilage* 2012; 20:  
544 949-956.
- 545 44. Leahy AA, Esfahani SA, Foote AT, Hui CK, Rainbow RS, Nakamura DS, et al. Analysis of the  
546 trajectory of osteoarthritis development in a mouse model by serial near-infrared fluorescence  
547 imaging of matrix metalloproteinase activities. *Arthritis Rheumatol* 2015; 67: 442-453.
- 548 45. Blom AB, van der Kraan PM, van den Berg WB. Cytokine targeting in osteoarthritis. *Curr Drug*  
549 *Targets* 2007; 8: 283-292.
- 550 46. Kraus VB, Birmingham J, Stabler TV, Feng S, Taylor DC, Moorman CT, 3rd, et al. Effects of  
551 intraarticular IL1-Ra for acute anterior cruciate ligament knee injury: a randomized controlled pilot  
552 trial (NCT00332254). *Osteoarthritis Cartilage* 2012; 20: 271-278.
- 553 47. Olson SA, Horne P, Furman B, Huebner J, Al-Rashid M, Kraus VB, et al. The role of cytokines in  
554 posttraumatic arthritis. *J Am Acad Orthop Surg* 2014; 22: 29-37.

- 555 48. Loeser RF, Collins JA, Diekman BO. Ageing and the pathogenesis of osteoarthritis. *Nat Rev*  
556 *Rheumatol* 2016; 12: 412-420.
- 557 49. Chevalier X, Eymard F, Richette P. Biologic agents in osteoarthritis: hopes and disappointments.  
558 *Nature Reviews Rheumatology* 2013; 9: 400.
- 559 50. Hwang HS, Park IY, Hong JI, Kim JR, Kim HA. Comparison of joint degeneration and pain in  
560 male and female mice in DMM model of osteoarthritis. *Osteoarthritis Cartilage* 2021.
- 561 51. Ma HL, Blanchet TJ, Peluso D, Hopkins B, Morris EA, Glasson SS. Osteoarthritis severity is sex  
562 dependent in a surgical mouse model. *Osteoarthritis Cartilage* 2007; 15: 695-700.
- 563 52. Arendt EA, Agel J, Dick R. Anterior cruciate ligament injury patterns among collegiate men and  
564 women. *J Athl Train* 1999; 34: 86-92.
- 565 53. Bram JT, Magee LC, Mehta NN, Patel NM, Ganley TJ. Anterior Cruciate Ligament Injury  
566 Incidence in Adolescent Athletes: A Systematic Review and Meta-analysis. *Am J Sports Med*  
567 2020: 363546520959619.
- 568 54. Agel J, Arendt EA, Bershadsky B. Anterior cruciate ligament injury in national collegiate athletic  
569 association basketball and soccer: a 13-year review. *Am J Sports Med* 2005; 33: 524-530.
- 570 55. Zhang X, Deng XH, Song Z, Croen B, Carballo CB, Album Z, et al. Matrix Metalloproteinase  
571 Inhibition With Doxycycline Affects the Progression of Posttraumatic Osteoarthritis After Anterior  
572 Cruciate Ligament Rupture: Evaluation in a New Nonsurgical Murine ACL Rupture Model. *Am J*  
573 *Sports Med* 2020; 48: 143-152.
- 574 56. Hamers FP, Lankhorst AJ, van Laar TJ, Veldhuis WB, Gispen WH. Automated quantitative gait  
575 analysis during overground locomotion in the rat: its application to spinal cord contusion and  
576 transection injuries. *J Neurotrauma* 2001; 18: 187-201.
- 577 57. Murphy MP, Koepke LS, Lopez MT, Tong X, Ambrosi TH, Gulati GS, et al. Articular cartilage  
578 regeneration by activated skeletal stem cells. *Nat Med* 2020; 26: 1583-1592.
- 579 58. Kotelsky A, Carrier JS, Buckley MR. Real-time Visualization and Analysis of Chondrocyte Injury  
580 Due to Mechanical Loading in Fully Intact Murine Cartilage Explants. *J Vis Exp* 2019.

- 581 59. Kotelsky A, Woo CW, Delgadillo LF, Richards MS, Buckley MR. An Alternative Method to  
582 Characterize the Quasi-Static, Nonlinear Material Properties of Murine Articular Cartilage. *J*  
583 *Biomech Eng* 2018; 140: 0110071-0110079.
- 584 60. Maas SA, Ellis BJ, Ateshian GA, Weiss JA. FEBio: finite elements for biomechanics. *J Biomech*  
585 *Eng* 2012; 134: 011005.
- 586 61. Glasson SS, Chambers MG, Van Den Berg WB, Little CB. The OARSI histopathology initiative -  
587 recommendations for histological assessments of osteoarthritis in the mouse. *Osteoarthritis*  
588 *Cartilage* 2010; 18 Suppl 3: S17-23.
- 589 62. Berke IM, Jain E, Yavuz B, McGrath T, Chen L, Silva MJ, et al. NF-kappaB-mediated effects on  
590 behavior and cartilage pathology in a non-invasive loading model of post-traumatic osteoarthritis.  
591 *Osteoarthritis Cartilage* 2021; 29: 248-256.
- 592 63. Bigoni M, Sacerdote P, Turati M, Franchi S, Gandolla M, Gaddi D, et al. Acute and late changes  
593 in intraarticular cytokine levels following anterior cruciate ligament injury. *Journal of Orthopaedic*  
594 *Research* 2013; 31: 315-321.
- 595 64. Guilak F, Erickson GR, Ting-Beall HP. The Effects of Osmotic Stress on the Viscoelastic and  
596 Physical Properties of Articular Chondrocytes. *Biophysical Journal* 2002; 82: 720-727.
- 597 65. Fitzgerald JB, Jin M, Dean D, Wood DJ, Zheng MH, Grodzinsky AJ. Mechanical compression of  
598 cartilage explants induces multiple time-dependent gene expression patterns and involves  
599 intracellular calcium and cyclic AMP. *Journal of Biological Chemistry* 2004; 279: 19502-19511.
- 600 66. Ng L, Hung H-H, Sprunt A, Chubinskaya S, Ortiz C, Grodzinsky A. Nanomechanical properties of  
601 individual chondrocytes and their developing growth factor-stimulated pericellular matrix. *Journal*  
602 *of Biomechanics* 2007; 40: 1011-1023.
- 603 67. Perera PM, Wypasek E, Madhavan S, Rath-Deschner B, Liu J, Nam J, et al. Mechanical signals  
604 control SOX-9, VEGF, and c-Myc expression and cell proliferation during inflammation via  
605 integrin-linked kinase, B-Raf, and ERK1/2-dependent signaling in articular chondrocytes. *Arthritis*  
606 *Res Ther* 2010; 12: R106.
- 607 68. Li Q, Han B, Wang C, Tong W, Wei Y, Tseng WJ, et al. Decorin Mediates Cartilage Matrix  
608 Degeneration and Fibrillation in Post-Traumatic Osteoarthritis. *Arthritis Rheumatol* 2020.

- 609 69. Angeby Moller K, Aulin C, Baharpoor A, Svensson CI. Pain behaviour assessments by gait and  
610 weight bearing in surgically induced osteoarthritis and inflammatory arthritis. *Physiol Behav* 2020;  
611 225: 113079.
- 612 70. Irie K, Uchiyama E, Iwaso H. Intraarticular inflammatory cytokines in acute anterior cruciate  
613 ligament injured knee. *The Knee* 2003; 10: 93-96.
- 614 71. Doyran B, Tong W, Li Q, Jia H, Zhang X, Chen C, et al. Nanoindentation modulus of murine  
615 cartilage: a sensitive indicator of the initiation and progression of post-traumatic osteoarthritis.  
616 *Osteoarthritis Cartilage* 2017; 25: 108-117.
- 617 72. Pragnere S, Boulocher C, Pollet O, Bosser C, Levillain A, Cruel M, et al. Mechanical alterations of  
618 the bone-cartilage unit in a rabbit model of early osteoarthrosis. *J Mech Behav Biomed Mater*  
619 2018; 83: 1-8.
- 620 73. Kleemann RU, Krockner D, Cedraro A, Tuischer J, Duda GN. Altered cartilage mechanics and  
621 histology in knee osteoarthritis: relation to clinical assessment (ICRS Grade). *Osteoarthritis*  
622 *Cartilage* 2005; 13: 958-963.
- 623 74. Guilak F, Ratcliffe A, Lane N, Rosenwasser MP, Mow VC. Mechanical and biochemical changes  
624 in the superficial zone of articular cartilage in canine experimental osteoarthritis. *J Orthop Res*  
625 1994; 12: 474-484.
- 626 75. Chen AC, Bae WC, Schinagl RM, Sah RL. Depth- and strain-dependent mechanical and  
627 electromechanical properties of full-thickness bovine articular cartilage in confined compression. *J*  
628 *Biomech* 2001; 34: 1-12.
- 629 76. Schinagl RM, Gurskis D, Chen AC, Sah RL. Depth-dependent confined compression modulus of  
630 full-thickness bovine articular cartilage. *J Orthop Res* 1997; 15: 499-506.
- 631 77. Pulai JI, Chen H, Im HJ, Kumar S, Hanning C, Hegde PS, et al. NF-kappa B mediates the  
632 stimulation of cytokine and chemokine expression by human articular chondrocytes in response  
633 to fibronectin fragments. *J Immunol* 2005; 174: 5781-5788.
- 634 78. Charlier E, Deroyer C, Neuville S, Plener Z, Malaise O, Ciregia F, et al. Toward diagnostic  
635 relevance of the  $\alpha V\beta 5$ ,  $\alpha V\beta 3$ , and  $\alpha V\beta 6$  integrins in OA: expression within human cartilage and  
636 spinal osteophytes. *Bone Research* 2020; 8: 35.

- 637 79. Wang Q, Onuma K, Liu C, Wong H, Bloom MS, Elliott EE, et al. Dysregulated integrin  $\alpha V\beta 3$  and  
638 CD47 signaling promotes joint inflammation, cartilage breakdown, and progression of  
639 osteoarthritis. *JCI Insight* 2019; 4.
- 640 80. Lee W, Nims RJ, Savadipour A, Zhang Q, Leddy HA, Liu F, et al. Inflammatory signaling  
641 sensitizes Piezo1 mechanotransduction in articular chondrocytes as a pathogenic feed-forward  
642 mechanism in osteoarthritis. *Proc Natl Acad Sci U S A* 2021; 118.
- 643 81. Jones RC, Heegde FT, Jackson TR, O'Brien M, Board TN, Richardson SM, et al. Piezo1  
644 expression is increased in response to non-invasive impact of mouse knee joint. *Osteoarthritis  
645 and Cartilage* 2018; 26: S113-S114.